Table lists

TableS1. Dihedral angles (°) and bond lengths (Å) of experimental dyes in the solvent of THF.

		Mjs2		Bjs2	
Dihedral angles (°)	D1-Pi	C8-C1-N45-C46	-34.4	C10-C1-N45-C46	80.2
	D2-Pi	C8-C1-C30-C32	35.7	C10-C1-C30-C36	-31.9
	M/B-Pi	C23-C4-C80-C86	90.3	C13-C12-C82-C98	65.9
	A(G)-Pi	C20-C3-C31-C65	0.4	C18-C3-C31-C66	0.1
	A(H)-Pi	C20-C3-C71-C76	32.1	C18-C3-C71-C76	-31.1
Bond length (Å)	d1	N45-C34	1.430	N45-C34	1.429
	d2	C30-C1	4.063	C30-C1	4.061
	d3	C3-C31	4.051	C3-C31	4.050
	d4	C64-C71	1.478	C64-C71	1.478

Table S2. Vertical excitation energy (eV), absorption peak (nm), main electron transitions and oscillator strengths (*f*) of investigated dye@TiO_2 composites.

Dye	State	E(eV)	λ_{max}(nm)	*f*	CI(main)
Mjs2@TiO_2	1	1.8769	660.58	1.3653	H→L+1(0.59)
	2	2.1156	586.05	0.0074	H-2→L+1(0.49)
	3	2.5478	486.63	0.4813	H-1→L+1(0.37)
	4	2.8792	430.62	2.3694	H-2→L+9(0.48)
	5	2.9939	414.12	1.2407	H-2→L+1(0.44)
	6	3.0630	404.78	0.0069	H-3→L+1(0.42)
	7	3.1221	397.12	0.0757	H-1→L+1(0.38)
	8	3.2231	384.67	0.0021	H→L(0.66)
Bjs2@TiO_2	1	1.8991	652.87	1.3421	H→L+1(0.59)
	2	2.0905	593.09	0.0740	H-2→L+1(0.50)
	3	2.5541	485.43	0.6071	H-1→L+1(0.34)
	4	2.8338	437.52	2.3279	H-2→L+9(0.47)
	5	2.9942	414.09	1.3160	H→L+9(0.53)
	6	3.0626	404.83	0.0154	H-3→L+1(0.39)
	7	3.1445	394.29	0.0653	H-1→L+1(0.34)
	8	3.2120	386.00	0.0007	H→L(0.66)
B-Dye1@TiO_2	1	1.8943	654.51	1.3591	H→L+1(0.58)
	2	2.0886	593.62	0.0752	H-2→L+1(0.51)
	3	2.5505	486.12	0.5922	H-1→L+1(0.35)
	4	2.8243	438.99	2.2610	H-2→L+10(0.45)
	5	2.9912	414.50	1.3801	H→L+10(0.50)
	6	3.0566	405.63	0.0084	H-3→L+1(0.37)
	7	3.1379	395.11	0.0854	H-1→L+1(0.35)
	8	3.2072	386.58	0.0011	H→L(0.65)
B-Dye2@TiO_2	1	1.8994	652.75	1.3418	H→L+1(0.56)
	2	2.0836	595.05	0.0891	H-1→L+1(0.52)
	3	2.5438	487.39	0.5982	H-2→L+1(0.35)
	4	2.8382	436.84	2.2236	H-1→L+9(0.47)
	5	2.9986	413.47	1.2952	H→L+9(0.51)
	6	3.0609	405.06	0.0074	H-3→L+1(0.38)
	7	3.1376	395.15	0.1006	H-2→L+1(0.35)
	8	3.2398	382.70	0.0009	H→L(0.64)

Table S3. Vertical excitation energy (eV), absorption peak (nm), electron transitions, oscillator strengths (f), and light harvesting efficiency (*LHE*) of investigated dyes@TiO_2.

Dye	Energy	λ	*f*	*LHE*
Mjs2@TiO_2	1.8769	660.58	1.3653	0.9568
Bjs2@TiO_2	1.8991	652.87	1.3421	0.9546
B-Dye1@TiO_2	1.8943	654.51	1.3591	0.9563
B-Dye2@TiO_2	1.8994	652.75	1.3418	0.9545

TableS4. Dihedral angles (°) and bond lengths (Å) of design dyes in the solvent of THF.

		B-Dye1		B-Dye2	
Dihedral angles (°)	D1-Pi	C10-C1-N45-C46	80.6	C10-C1-N45-C46	80.7
	D2-Pi	C10-C1-C30-C36	-30.8	C10-C1-C30-C36	-30.8
	M/B-Pi	C13-C12-C82-C98	66.1	C13-C12-C82-C98	66.0
	A(G)-Pi	C18-C3-C31-C66	-0.7	C18-C3-C31-C66	-0.1
	A(H)-Pi	C18-C3-C71-C76	-32.6	C18-C3-C71-C76	-36.2
Bond length (Å)	d1	N45-C34	1.429	N45-C34	1.429
	d2	C30-C1	4.061	C30-C1	4.061
	d3	C3-C31	4.043	C3-C31	4.042
	d4	C64-C71	1.477	C64-C71	1.478

Table S5. The contribution for holes and electrons by different parts (*D, π, A*) of investigated single molecules.

Dye		hole	electron
Mjs2	Donor	10.75%	8.06%
	π-bridge	83.44%	85.27%
	Acceptor	5.81%	6.67%
Bjs2	Donor	11.80%	8.92%
	π-bridge	82.42%	84.26%
	Acceptor	5.78%	6.82%
B-Dye1	Donor	12.83%	7.98%
	π-bridge	80.11%	80.37%
	Acceptor	7.06%	11.64%
B-Dye2	Donor	15.52%	7.72%
	π-bridge	78.75%	80.58%
	Acceptor	5.73%	11.70%

Table S6. The calculated electronic transition data in terms of excitation energies (E), band wavelengths (λ), oscillator strengths (*f*), the main transition mode and probability of electron in THF on CPCM model.

Dye	State	E (eV)	λ_{max} (nm)	*f*	CI (main)
B-Dye1	1	1.8971	653.56	1.2545	H→L (0.61)
	2	2.0894	593.38	0.0714	H-2→L (0.54)
	3	2.5511	486.00	0.6158	H-1→L (0.37)
	4	2.8611	433.34	2.0994	H-2→L+1 (0.51)
	5	2.9896	414.71	1.3374	H→L+1 (0.54)
	6	3.0702	403.83	0.0100	H-3→L (0.43)
	7	3.1514	393.42	0.0447	H-1→L (0.36)
	8	3.4028	364.36	0.0046	H-1→L+3 (0.31)
B-Dye2	1	1.9010	652.20	1.2430	H→L (0.60)
	2	2.0867	594.17	0.0832	H-1→L (0.50)
	3	2.5445	487.26	0.6048	H-2→L (0.33)
	4	2.8724	431.64	2.0589	H-1→L+1 (0.48)
	5	2.9977	413.60	1.3188	H→L+1 (0.54)
	6	3.0748	403.22	0.0374	H-3→L (0.45)
	7	3.1454	394.18	0.0641	H→L+2 (0.36)
	8	3.4223	362.28	0.0083	H→L+3 (0.30)

Table S7. The simulated Ti-O distances (Å) between TiO_2 and dye of investigated dye/TiO_2 composites as well as interaction energy (kcal/mol).

Dye	Bond length1 (Å)	Bond length2 (Å)	Energy (kcal/mol)
Mjs2@TiO_2	2.07321	2.06630	-12.52
Bjs2@TiO_2	2.07594	2.06434	-12.76
B-Dye1@TiO_2	2.08005	2.06603	-12.46
B-Dye2@TiO_2	2.08521	2.06229	-15.23

Figure lists

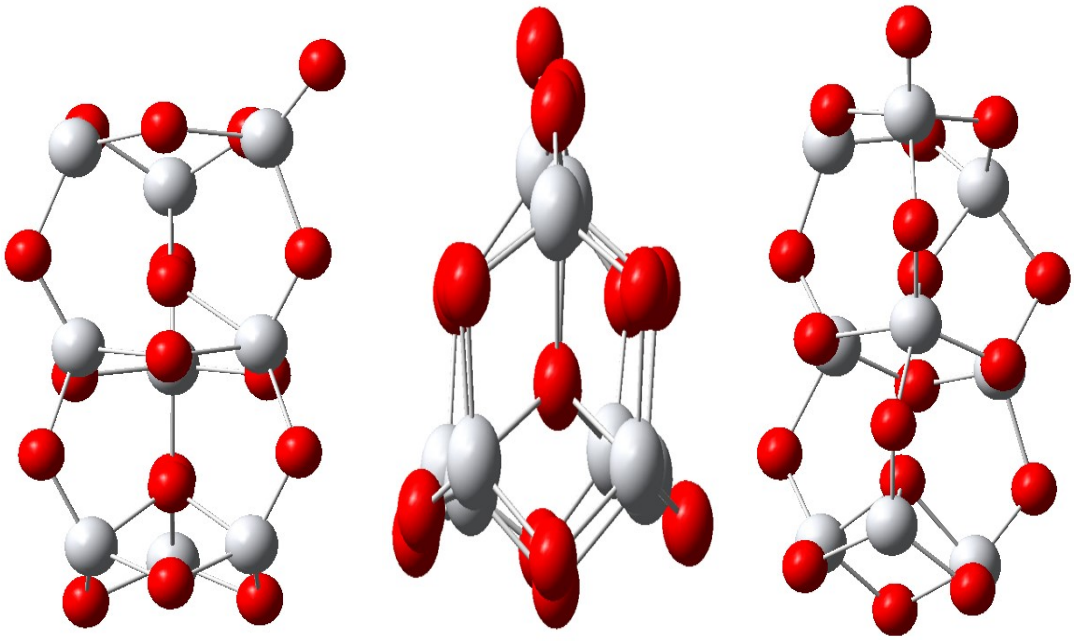

(a) Front view (b) Vertical view (c) Side view

Figure.S1 The geometry structure of optimized $(TiO_2)_9$ cluster. (a) The front view of the optimized structure. (b) The vertical view of the optimized structure. (c) The side view of the optimized structure.

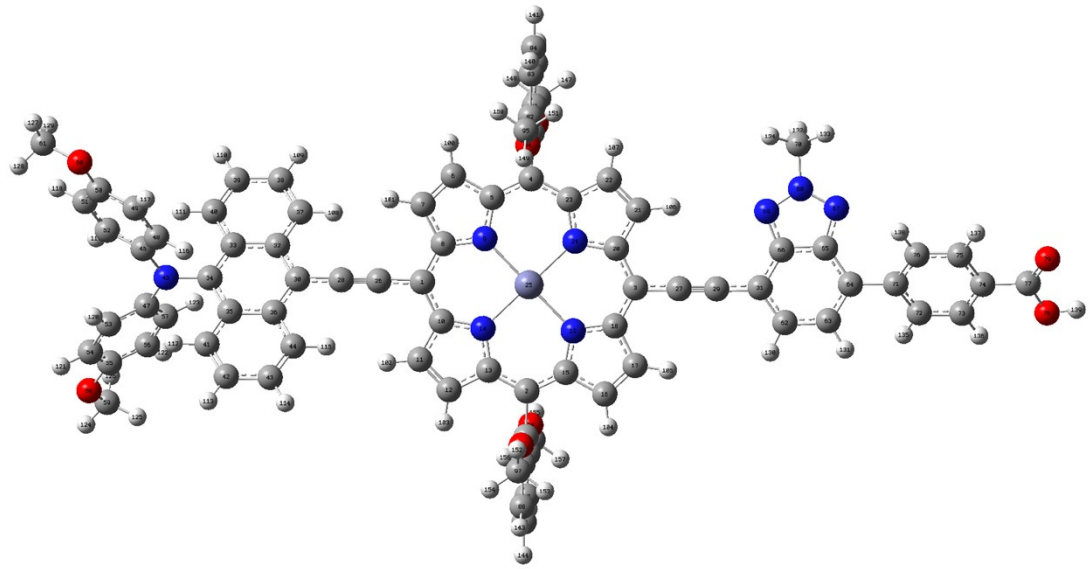

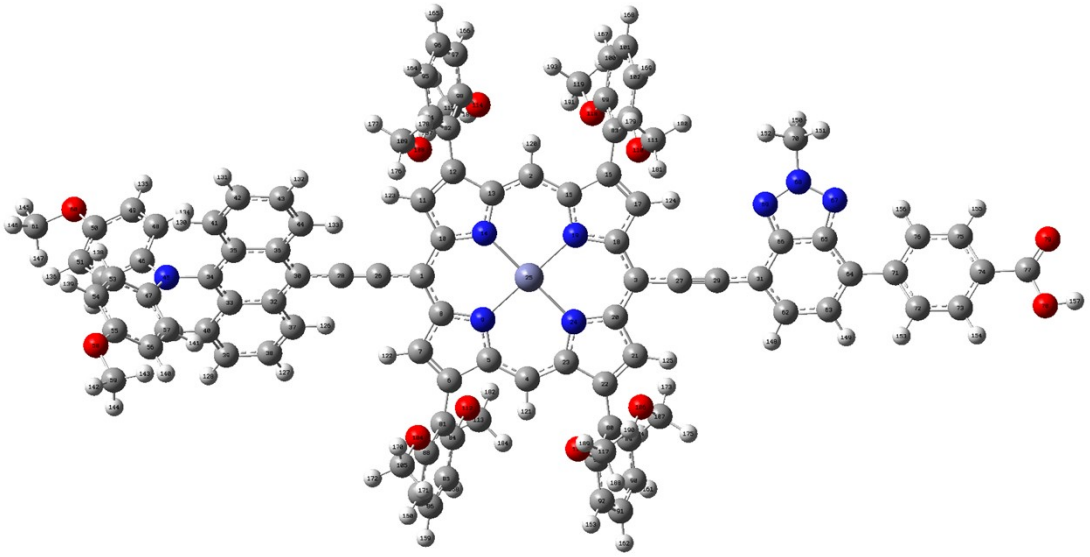

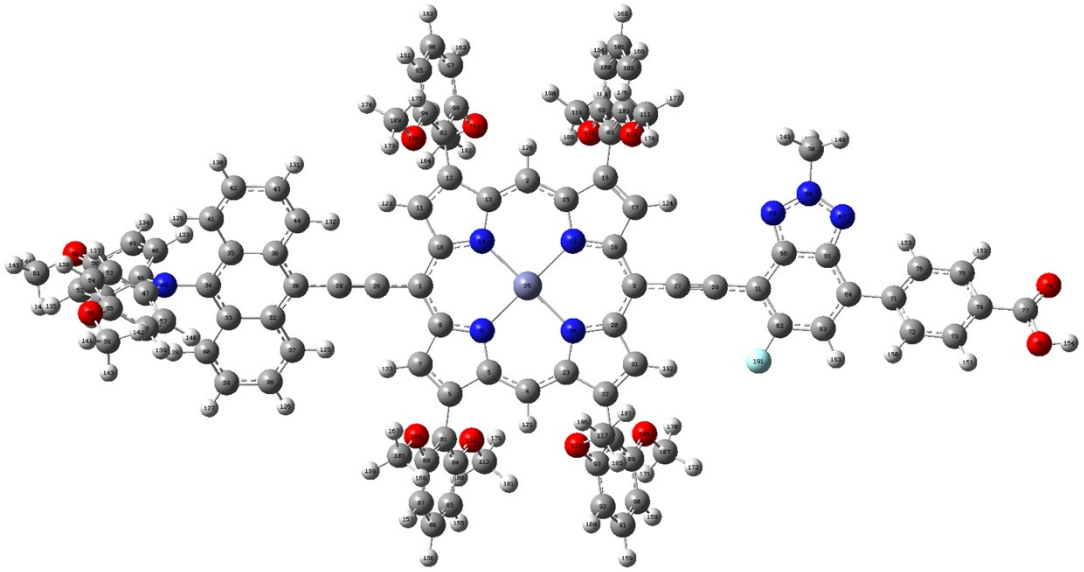

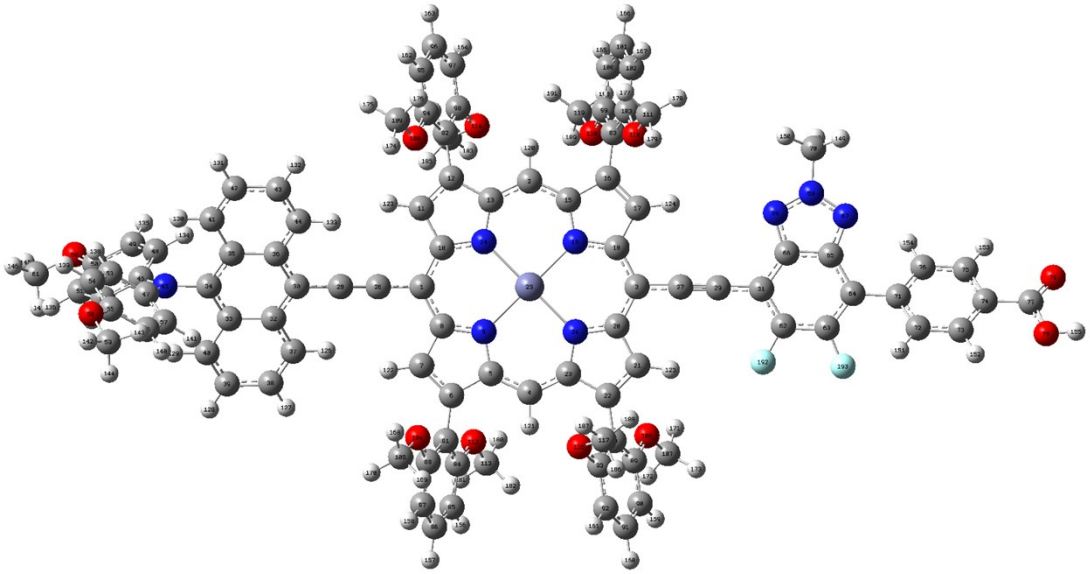

Figure.S2 The geometric configuration and atom labels of all investigated dye molecules (Mjs2, Bjs2, B-Dye1, B-Dye2).

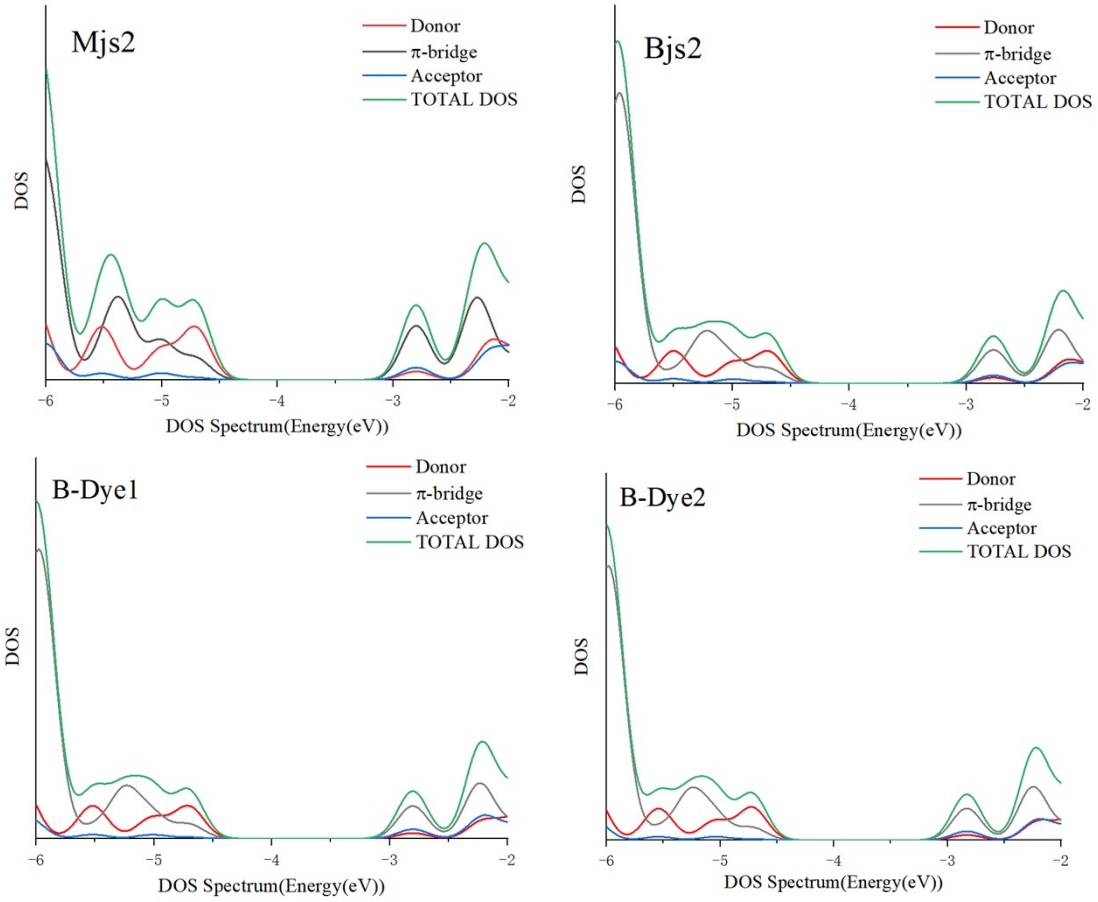

Figure.S3 Total density of states (TOTAL DOS) and projected density of states (PDOS) of the investigated dyes.

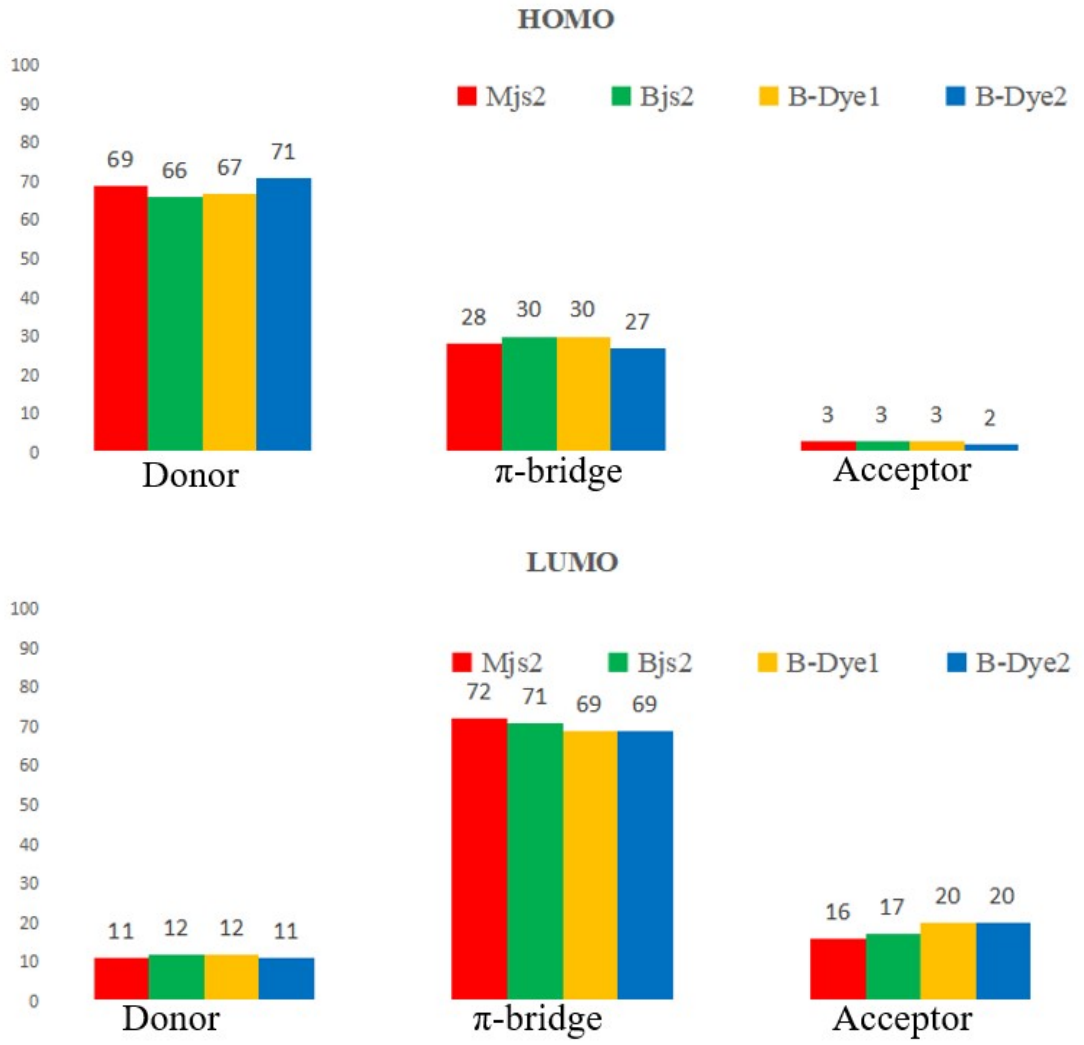

Figure.S4 Molecular orbital compositions of individual groups (D, π, A) in HOMO and LUMO of the investigated dyes.

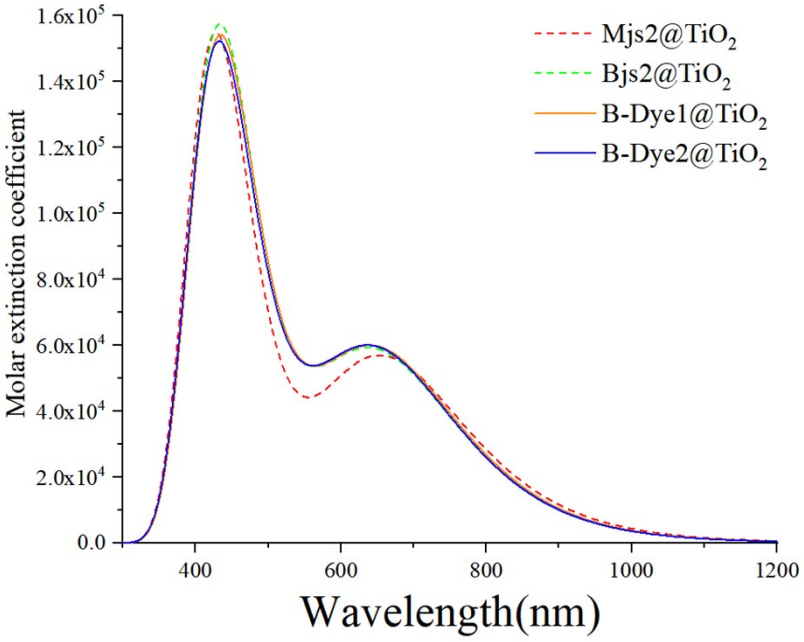

Figure.S5 The UV-Vis absorption spectra of dye@TiO_2 at the CAM-B3LYP/6-31G(d) level in THF. For Zn atom only LANL2DZ basis set was used.

Dye	HOMO-2	HOMO-1	LUMO+1	LUMO+2
Mjs2@TiO_2	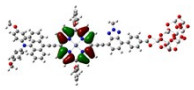	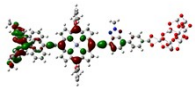	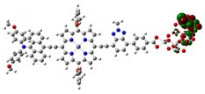	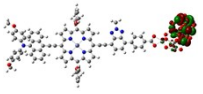
Bjs2@TiO_2	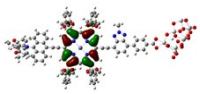	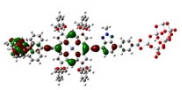	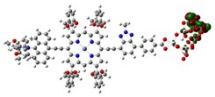	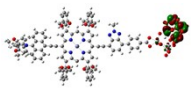
B-Dye1@TiO_2	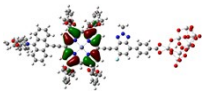	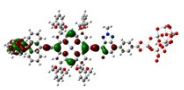	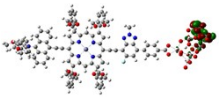	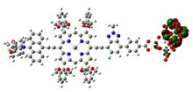
B-Dye2@TiO_2	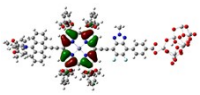	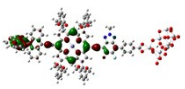	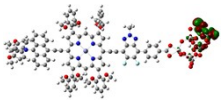	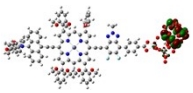

Figure.S6 The frontier molecular orbitals (HOMO-2, HOMO-1, LUMO+1, LUMO+2) diagrams of the dye@TiO_2 in THF.

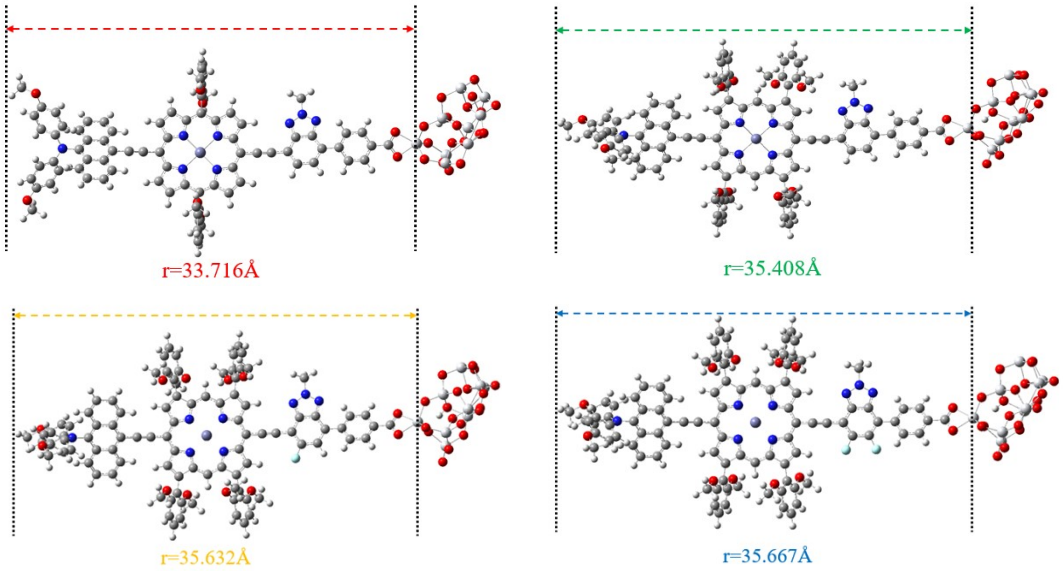

Figure.S7 The optimized geometries of dye@TiO_2, and the illustration of electron recombination distance.